2nd URSI AT-RASC, Gran Canaria, 28 May – June 2018

Numerical Investigation of Nano-Cavities for Optimal Power Absorption in Solar Cells

Barışcan Karaosmanoğlu*(1), Ulaş Topçuoğlu(1), Emre Tuygar(1), and Özgür Ergül(1)
(1) Department of Electrical and Electronics Engineering, Middle East Technical University, Ankara, Turkey
bariscankaraosmanoglu@gmail.com

Abstract

We present a numerical study of nano-cavities used in solar cells for energy harvesting, by employing surface integral equations based on Maxwell's equations in the frequency domain and an efficient solver based on the multilevel fast multipole algorithm (MLFMA). With the three-dimensional modeling of surfaces, we obtain accurate results to evaluate the performances of different structures for improved power absorption in solar cells. This paper includes a brief description of the developed solver and initial numerical examples on various solar cells involving inverted pyramids and spherical cavities.

1 Introduction

There is a well-established literature on solar cells [1]–[10], including the development of alternative geometries, materials, and configurations to improve their efficiency. Numerical investigation of solar cells supports experimental studies in the direction of cost-efficient and energy-efficient structures [5]–[7]. These numerical studies involve circuit-based models, asymptotic techniques, statistical techniques, particle-based methods, and volumetric wave-based methods (particularly finite-difference time-domain method). On the other hand, many solar-cell scenarios involve only several different materials and details proportional to operating wavelengths, which can be formulated efficiently and accurately with surface integral equations derived directly from Maxwell's equations. This is particularly the case when solar-cell surfaces, as the most critical geometric parameters, need to be designed and analyzed.

In this contribution, we present numerical analysis of nano-cavities in solar cells using surface integral equations. Surfaces and interfaces between different media are modeled in three-dimensional space and discretized with the Rao-Wilton-Glisson (RWG) functions on small triangular domains. The derived dense matrix equations are solved iteratively, while the matrix-vector multiplications are performed efficiently by using the multilevel fast multipole algorithm (MLFMA). This paper includes the initial results on the numerical simulations that lead to accurate and important information on the characteristics of different realistic structures. The numerical setup is suitable for arbitrary geometries, which may enable the geometric optimization of nano-cavities for improved performances.

2 Brief Description of the Numerical Solver

For numerical simulations of solar cells, we consider surface formulations in the frequency domain assuming time-harmonic sources. Materials are represented by complex permittivity values. Among alternative formulations, the electric-magnetic current combined-field integral equation (JMCFIE) is preferred [11]. Surfaces and interfaces are discretized by using triangles, on which the RWG functions are defined to expand tangential electric and magnetic fields. Matrix equations are solved iteratively via Krylov-subspace algorithms, employing MLFMA for fast matrix-vector multiplications. For the examples presented in this paper, the number of unknowns is in the range from 45,234 to 1,767,516. Near-zone electromagnetic interactions are computed via singularity extraction and Gaussian quadrature rules. Far-zone interactions are computed via the expansion of the Green's function in terms of plane waves with angular sampling based on excess bandwidth formula. Field up-sampling and down-sampling are performed via Lagrange interpolation. Accuracy of solutions is verified by testing the extinction theorem as well as by perform-

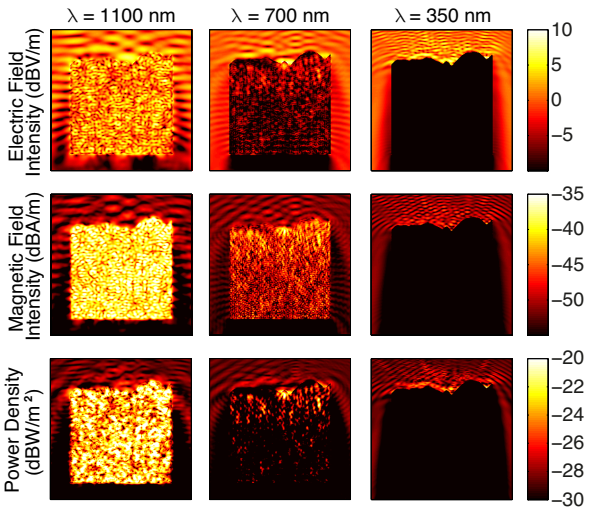

Figure 1. The electric field intensity (dBV/m), the magnetic field intensity (dBA/m), and the power density (dBW/m^2) in the vicinity of a c-Si block with a corrugated surface excited at different frequencies.

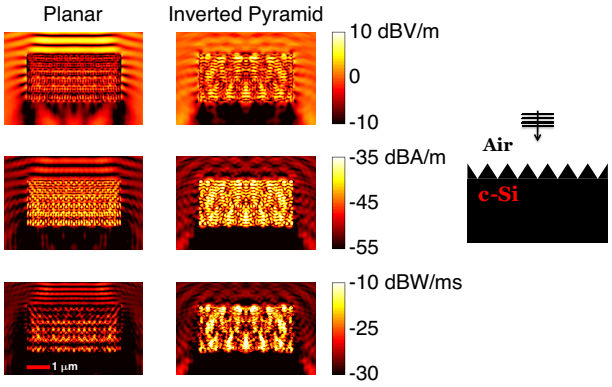

Figure 2. The electric field intensity (dBV/m), the magnetic field intensity (dBA/m), and the power density (dBW/m^2) in the vicinity of $4.2 \times 4.2 \times 2.0$ μm c-Si slabs excited at 375 THz. The efficiency improves when inverted pyramids are used, in comparison to the planar case.

ing mesh convergence. Once the tangential fields at interfaces are found, the equivalence theorem is used by radiating sources in homogeneous media to find electric and magnetic fields, as well as power density distributions, everywhere. More information on the numerical implementation can be found in [12].

3 Numerical Investigation of Nano-Cavities

In the following subsections, we consider several different factors, i.e., frequency dependency of materials, cavity geometries, and matching layers, that are critical for solar cells. In all results, the excitation is modeled as a plane wave propagating directly onto the active surfaces of the investigated solar cells.

3.1 Frequency-Dependency of Materials

One of the most common materials for building solar cells is crystalline silicon (c-Si). While it has many favorable properties, c-Si has a relatively large contrast values (with respect to air), making it less effective and efficient for harvesting solar energy at some frequencies. As the frequency increases, the real part of the permittivity increases, deteriorating the match between air and solar cell. At the same time, the loss (represented by the imaginary part of the permittivity) also increases so that the absorption occurs mainly in the vicinity of the interfaces. As an example, Fig. 1 presents the electric field intensity (in dBV/m), the magnetic field intensity (in dBA/m), and the power density (in dBW/m^2) for a c-Si block excited at different frequencies. The cross section of the block is a 5.0×5.0 μm square, while its top (illuminated) surface is randomly corrugated. When the wavelength is 1100 nm (frequency is approximately 273 THz), the electromagnetic radiation effectively penetrates into the block. At this frequency, the relative permittivity of c-Si is taken as $12.54 + 0.0043i$. When the wavelength is 700 nm and the frequency is approximately 428 THz, the relative permittivity of c-Si becomes

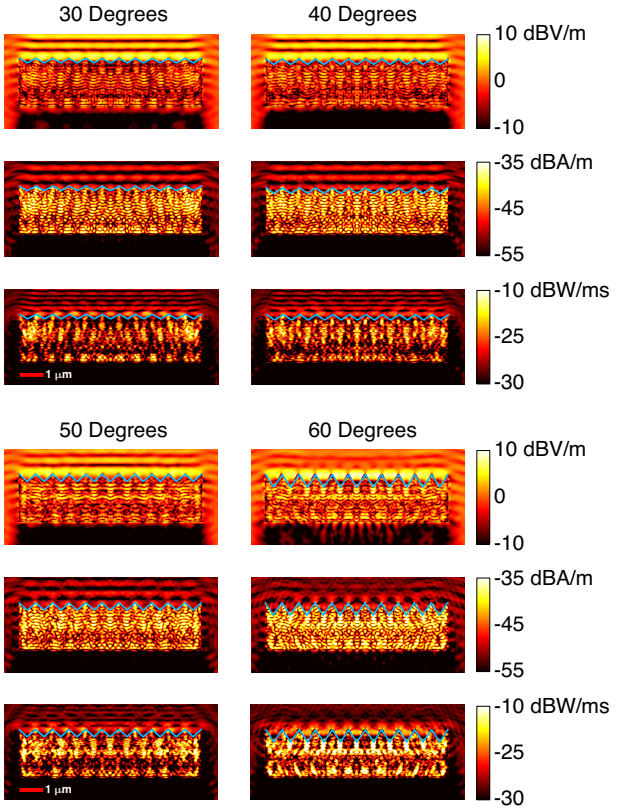

Figure 3. The electric field intensity (dBV/m), the magnetic field intensity (dBA/m), and the power density (dBW/m^2) in the vicinity of $7.7 \times 7.7 \times 2.0$ μm c-Si slabs excited at 375 THz. Inverted pyramids with different angles (30°, 40°, 50°, and 60°) are used.

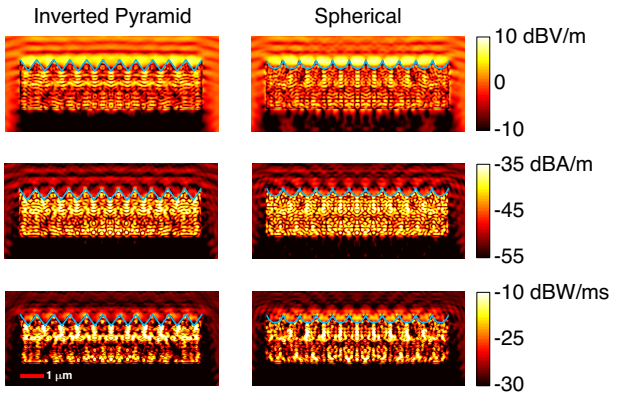

Figure 4. The electric field intensity (dBV/m), the magnetic field intensity (dBA/m), and the power density (dBW/m^2) in the vicinity of $7.7 \times 7.7 \times 2.0$ μm c-Si slabs excited at 375 THz. The slab with spherical cavities (right) is compared to the one with inverted pyramids (54.7° angle).

approximately $14.32 + 0.0921i$. In this case, the mismatch increases slightly, but the higher loss leads a quick decay inside the block. Finally, when the wavelength becomes 350 nm (at approximately 857 THz) and the relative permittivity becomes approximately $20.97 + 32.88i$, the mismatch

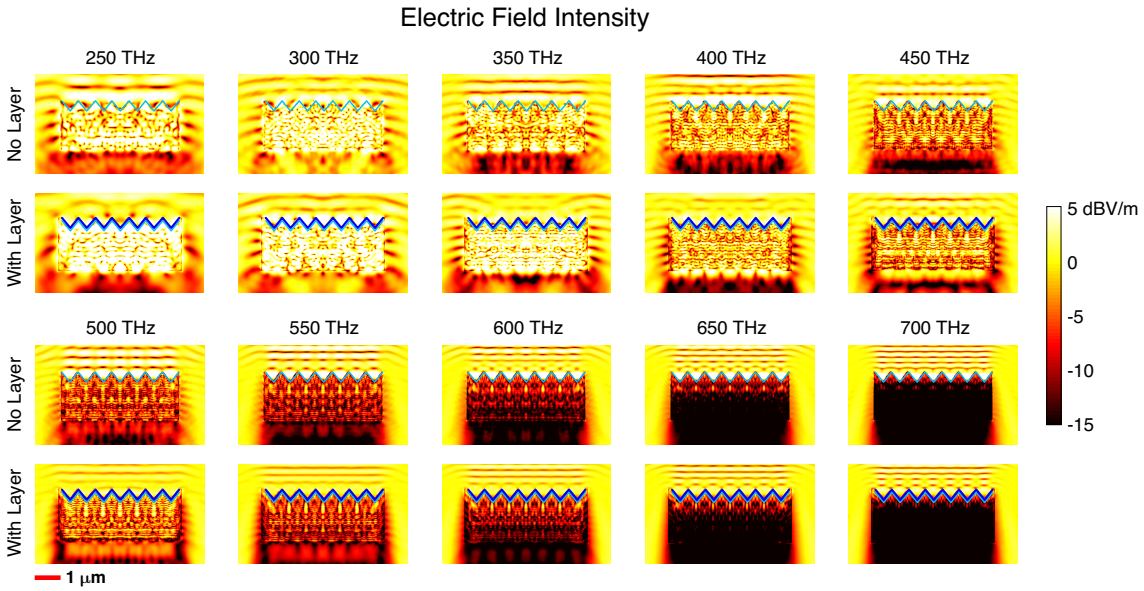

Figure 5. The electric field intensity (dBV/m) in the vicinity of c-Si slabs with inverted pyramids excited at different frequencies. In addition to the pure c-Si slab, results for a c-Si slab covered with a thin layer of Si_3N_4 is considered.

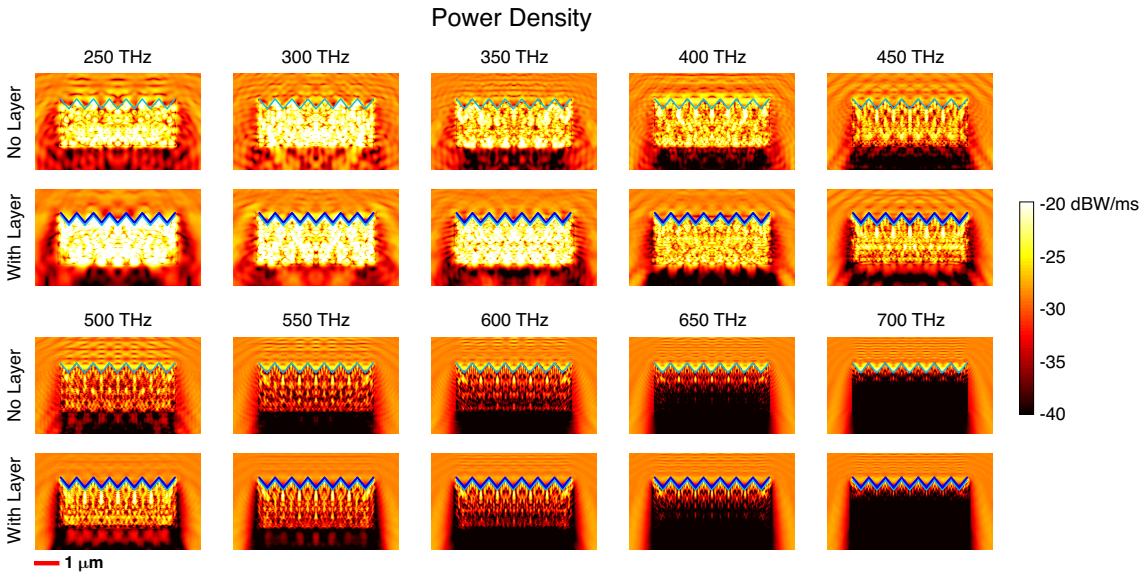

Figure 6. The power density (dBW/m^2) in the vicinity of c-Si slabs with inverted pyramids excited at different frequencies. In addition to the pure c-Si slab, results for a c-Si slab covered with a thin layer of Si_3N_4 is considered.

further increases, while most of the absorption occurs just beneath the surface.

3.2 Reducing Mismatch via Inverted Pyramids

Using cavities in the shape of inverted pyramids is a well-known technique [9] to improve the efficiency of solar cells. As an example, Fig. 2 presents field and power density distributions for $4.2 \times 4.2 \times 2.0$ μm c-Si slabs. In addition to the one with a planar top surface, a slab on which 6×6 inverted pyramids are opened is considered. The pyramid angle is selected as 54.7°, which usually leads efficient results [9]. The slabs are excited at 375 THz from the top. The relative permittivity of c-Si at this frequency is $13.65 + 0.0484i$. It can be observed that the pyramids significantly improve the penetration into the slab, while reducing reflection from the top (illuminated) interface.

Inverted-pyramid cavities are effective; but their geometric parameters are extremely important and the performance of a solar cell strictly depends on them. As an example, Figs. 3 and 4 present field and power density distributions for $7.7 \times 7.7 \times 2.0$ μm c-Si slabs. Once again, the frequency is set to 375 THz ($13.65 + 0.0484i$ relative permittivity). On the top surfaces, 7×7 inverted pyramids with different angles, i.e., 30°, 40°, 50°, and 60°, are used. It can be observed that solar-cell characteristics change significantly

with the pyramid angle. For smaller angles (e.g., 30° and 40°), the reflection is significant, which is visible as oscillatory variations (due to interference of incident and reflected waves) in the reflection region. As the angle increases to 50° and 60°, the electromagnetic power is trapped inside the cavities and the reflection is significantly reduced. These results verify the optimality of $50^\circ - 60^\circ$ for inverted pyramids.

3.3 Alternative Nano-Cavity Geometries

As shown in the literature, other kinds of nanostructures (e.g., metallic/plasmonic nanoparticles and nanowires [1]–[5],[10]) and nano-cavities [8] can be used to improve the efficiency of solar cells, while the performances may vary significantly. In order to demonstrate an alternative structure, which can perform as good as inverted pyramids at certain frequencies, Fig. 4 depicts a comparison involving $7.7 \times 7.7 \times 2.0$ μm c-Si slabs at 375 THz. In addition to inverted pyramids with 54.7° angle, we consider spherical nano-cavities opened on the top (excited) surface. We note that the diameter of the spheres is just below the wavelength, for which the cavities tend to resonate. It can be observed that two solar-cell structures in Fig. 6 behave almost the same with very good absorption characteristics.

3.4 Using Matching Layers

Since geometric improvements can be limited, matching layers can be used to further enhance the efficiency of solar cells. Particularly silicon nitride (Si_3N_4) is a common material to cover cell surfaces made of c-Si. As an example, Figs. 5 and 6 present the electric field intensity and the power density, respectively, in the vicinity of c-Si slabs from 250 THz to 700 THz. Inverted pyramids with 54.7° angle are used to improve the efficiency of solar cells. In addition to the pure c-Si slab, we consider the one covered with a thin Si_3N_4 layer. It can be observed that the absorption increases significantly (that can be deduced from the patterns in the reflection region, especially in the plots of electric field intensity) at most frequencies.

4 Concluding Remarks

Surface integral equations derived from Maxwell's equations are suitable for numerical analysis of solar cells. As shown in this paper, accurate solutions obtained by using a robust implementation provide essential information on different structures, particularly on the nano-cavities that are used for enhancing the efficiency solar cells. The flexibility of the developed implementation that allows for three-dimensional modeling makes optimizations possible, which will be addressed in a future publication.

5 Acknowledgements

This work was supported by the Scientific and Technical Research Council of Turkey (TUBITAK) under the Research Grant 114E498 and by the Turkish Academy of Sciences (TUBA) in the framework of the Young Scientist Award Program.

References

[1] H. R. Stuart and D. G. Hall, "Absorption enhancement in silicon-on-insulator waveguides using metal island films," *Appl. Phys. Lett.*, **69**, 16, October 1996, pp. 2327–2329.

[2] K.-Q. Peng, Y. Xu, Y. Wu, Y. Yan, S.-T. Lee, and J. Zhu, "Aligned single-crystalline Si nanowire arrays for photovoltaic applications," *Small*, **1**, 11, August 2005, pp. 1062–1067.

[3] S. Pillai, K. R. Catchpole, T. Trupke, and M. A. Green, "Surface plasmon enhanced silicon solar cells," *J. Appl. Phys.*, **101**, 9, May 2007.

[4] C. M. Hsu, S. T. Connor, M. X. Tang, and Y. Cui, "Wafer-scale silicon nanopillars and nanocones by Langmuir-Blodgett assembly and etching," *Appl. Phys. Lett.*, **93**, 13, October 2008.

[5] H. A. Atwater and A. Polman, "Plasmonics for improved photovoltaic devices," *Nat. Mater.*, **9**, February 2010, pp. 205–213.

[6] Z. Yu, A. Raman, and S. Fan, "Fundamental limit of nanophotonic light trapping in solar cells," *PNAS*, **107**, 41, October 2010, pp. 17491–17496.

[7] L. Cao, P. Fan, A. P. Vasudev, J. S. White, Z. Yu, W. Cai, J. A. Schuller, S. Fan, and M. L. Brongersma, "Semiconductor nanowire optical antenna solar absorbers," *Nano Lett.*, **10**, 2, January 2010, pp. 439–445.

[8] K.-Q. Peng, X. Wang, L. Li, X.-L. Wu, and S.-T. Lee, "High-performance silicon nanohole solar cells," **132**, 20, April 2010, pp. 6872–6873.

[9] A. Mavrokefalos, S. E. Han, S. Yerci, M. S. Branham, and G. Chen, "Efficient light trapping in inverted nanopyramid thin crystalline silicon membranes for solar cell applications," *Nano Lett.*, **12**, 6, May 2012, pp. 2792–2796.

[10] Y. Cui, D. van Dam, S. A. Mann, N. J. J. van Hoof, P. J. van Veldhoven, E. C. Garnett, E. P. A. M. Bakkers, and J. E. M. Haverkort, "Boosting solar cell photovoltage via nanophotonic engineering," *Nano Lett.*, **16**, 10, September 2016, pp. 6467–6471.

[11] Ö. Ergül, "Solutions of large-scale electromagnetics problems involving dielectric objects with the parallel multilevel fast multipole algorithm," *J. Opt. Soc. Am. A.*, **28**, 11, November 2011, pp. 2261–2268.

[12] A. Çekinmez, and B. Karaosmanoğlu, Ö. Ergül, "Integral-equation formulations of plasmonic problems in the visible spectrum and beyond," in *Dynamical Systems - Analytical and Computational Techniques.* InTech, 2017.